

Hydrophobic Hydration in Water–*tert*-Butyl Alcohol Solutions by Extended Depolarized Light Scattering

L. Comez,^{†,‡} M. Paolantoni,[§] L. Lupi,^{||} P. Sassi,[§] S. Corezzi,[‡] A. Morresi,[§] and D. Fioretto^{*,†,‡,⊥}

[†]IOM-CNR c/o Dipartimento di Fisica e Geologia, Università di Perugia, Via Pascoli, I-06123 Perugia, Italy

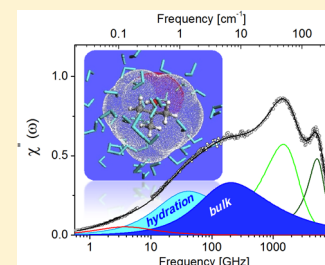
[‡]Dipartimento di Fisica e Geologia, Università di Perugia, Via Pascoli, I-06123 Perugia, Italy

[§]Dipartimento di Chimica, Biologia e Biotecnologie, Università di Perugia, Via Elce di Sotto 8, I-06123 Perugia, Italy

^{||}Department of Chemistry, The University of Utah, 315 South 1400 East, Salt Lake City, Utah 84112-0850, United States

[⊥]Centro di Eccellenza sui Materiali Innovativi Nanostrutturati (CEMIN), Università di Perugia, Via Elce di Sotto 8, I-06123 Perugia, Italy

ABSTRACT: Molecular dynamics and structural properties of water–*tert*-butyl alcohol (TBA) mixtures are studied as a function of concentration by extended depolarized light scattering (EDLS) experiments. The wide frequency range, going from fraction to several thousand GHz, explored by EDLS allows distinguishing TBA rotational dynamics from structural relaxation of water and intermolecular vibrational and librational modes of the solution. Contributions to the water relaxation originating from two distinct populations, i.e. hydration and bulk water, are clearly identified. The dynamic retardation factor of hydration water with respect to the bulk, $\xi \approx 4$, almost concentration independent, is one of the smallest found by EDLS among a variety of systems of different nature and complexity. This result, together with the small number of water molecules perturbed by the presence of TBA, supports the idea that hydrophobic simple molecules are less effective than hydrophilic and more complex molecules in perturbing the H-bond network of liquid water. At increasing TBA concentrations the average number of perturbed water molecules shows a pronounced decrease and the characteristic frequency of librational motions reduces significantly, both of which are results consistent with the occurrence of self-aggregation of TBA molecules.



I. INTRODUCTION

Hydrophobic hydration and aggregation play a key role in many biological processes, from assembling of membranes, to protein–ligand binding and protein folding.¹

Small solute molecules are usually selected as simple models to investigate the hydrophobic effects.² The most commonly investigated systems are the monohydric alcohols. Among these, the *tert*-butyl alcohol is widely studied—see, e.g., refs.^{3–5}—as it is one of the most soluble in water and with the largest hydrophobic group.

Experimental investigations at the molecular scale^{6–8} as well as numerical studies^{9–11} show subtle variations in the structure of water surrounding hydrophobic groups. Conversely, spectroscopic investigations show that hydrophobic hydration is responsible for a large variation in the dynamics of water. A slow-down of the dynamics of hydration water is usually reported, associated with either stronger H-bonds or excluded volume effects. Nevertheless, the extent of the retardation is still controversial. Femtosecond infrared spectroscopy of TBA and tetramethylurea suggests a slowing down of a few solvating water molecules by a factor $\xi > 4$.¹² These results are supported by femtosecond two-dimensional infrared spectroscopy,¹³ dielectric spectroscopy investigation,¹⁴ and ab initio Car–Parrinello MD simulations.¹⁵ On the contrary, classical MD simulations^{16–19} suggest a milder slow-down of the reorientational dynamics ($\xi < 2$) involving all the water molecules in the

first hydration shell. The results are in agreement with rotational correlation times measured by NMR.^{20–23}

The aim of the present work is to contribute to understanding the degree and the spatial extent of the perturbation induced by each TBA molecule on surrounding water. To this purpose, we use the extended depolarized light scattering technique (EDLS). This technique, originally introduced to study the dynamics of glass forming liquids,²⁴ has been recently applied successfully to study the dynamics of H-bond liquids²⁵ and the solvation of biologically relevant molecules.²⁶ The mechanisms of interaction of light with molecular motions is very complex, for this reason the possibility of comparing EDLS results with MD simulations is of great importance. Recently, molecular modeling of light scattering from fluids has been successfully developed by Ladanyi and co-workers^{27–29} and used to investigate the contribution from solute and solvent to EDLS spectra of water solutions.^{30,31} Water–TBA solutions are particularly suitable for light scattering experiments, since TBA has a very low anisotropic polarizability and the contribution from hydration water can be easily identified in the spectra. EDLS measure-

Special Issue: Branka M. Ladanyi Festschrift

Received: September 29, 2014

Revised: November 28, 2014

ments have been performed in the diluted condition, i.e. for TBA mole fractions up to $x = 0.05$. Depolarized low frequency Raman measurements have been extended up to $x = 0.1$. This is a concentration range where interesting anomalies were previously reported in water–TBA solutions. A first transition was reported by different techniques^{32–34} at the alcohol molar fraction $x \approx 0.025$, or even less,⁵ attributed to the clusterization of alcohol molecules. At higher concentrations ($x \approx 0.05$), a second transition was observed,³⁵ which has recently been attributed to the percolation of TBA clusters.^{11,36}

II. EXPERIMENT

EDLS experiments were carried out for water–TBA mixtures at $T = 20\text{ }^{\circ}\text{C}$ and for TBA mole fractions in the range $0 < x < 0.05$. Raman scattering experiments were carried out at the same temperature, for TBA concentrations up to $x = 0.1$. TBA was purchased by Sigma-Aldrich with purity >99% and dissolved without further purification into doubly distilled deionized water. Freshly prepared solutions were directly filtered into the optical quartz cell through filters with a $0.2\text{ }\mu\text{m}$ pore size. Depolarized (I_{VH}) spectra were acquired in the frequency range between 0.3 GHz and 30 THz by means of two different spectrometers: a Sandercock-type (3 + 3) pass tandem Fabry–Perot interferometer³⁷ in the range 0.3–200 GHz and an ISA Jobin–Yvon model U1000 double monochromator in the range 3 GHz–30 THz. More details on the experimental setup can be found in ref 38. The susceptibility spectrum $\chi''(\omega)$ was calculated as the ratio between $I_{\text{VH}}(\omega)$ and $[n(\omega) + 1]$, where $n(\omega)$ is the Bose–Einstein occupation number, namely $n(\omega) = \exp[(\hbar\omega/k_{\text{B}}T) - 1]^{-1}$.

III. RESULTS AND DISCUSSION

The susceptibility spectra of water–TBA solutions are reported in Figure 1. The high frequency (THz) part of the spectrum of pure water is characterized by three resonant peaks, which are assigned to intermolecular Raman modes. The H-bond bending ($\text{O}\cdots\text{O}\cdots\text{O}$ unit) gives rise to the broad peak at about 1.5 THz, the H-bond stretching ($\text{O}\cdots\text{O}$ unit) to the narrower peak at about 5.1 THz,³⁹ and librations to the broad bump in the 10–30 THz region. The spectra are normalized to this last feature,

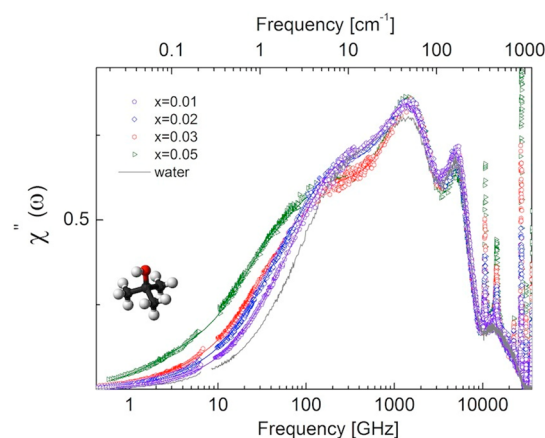


Figure 1. EDLS susceptibility (symbols) of water–TBA solutions at different concentrations, at $T = 20\text{ }^{\circ}\text{C}$. The solid lines represent the fitting curves described in the text. The experimental points around 7 GHz have been removed from the depolarized spectra due to a spurious contribution arising from the leakage of the polarizer.

which results to be less affected by the presence of the solute. On the opposite side, the low frequency shoulder of the spectrum of pure water is assigned to the structural relaxation of water.⁴⁰ It has been shown³⁹ that the major contribution to the scattering in this region comes from dipole–induced dipole (DID) effects. This indicates that fluctuations of optical polarizability in water are dominated by the translational dynamics, which is known to be strongly affected by the relaxation of the hydrogen bond network.^{29,41} This has recently been confirmed for water solutions of carbohydrates.³⁰

It can be seen from Figure 1 that addition of TBA is responsible for considerable variations of the spectrum, both in the low frequency (relaxations) and in the high frequency (resonant modes) region. Interestingly, the rotational diffusion of TBA gives rise to a spectral contribution in the 1–10 GHz region with amplitude very small with respect to that of pure water, as discussed in the next paragraph. Consequently, it is reasonable to attribute to hydration water the extra intensity well visible in the 10–100 GHz region. The existence of such a contribution, which has been revealed by EDLS experiments in many solutes of different nature and complexity,²⁶ has not been recognized by recent extensive MD simulations of depolarized spectra of peptide and protein solutions.^{42,43} On the other hand, these simulations have suggested the existence of a cross solute–solvent contribution with relaxation time very close to that of the solute, which has never been observed experimentally. In this respect, the very clean, water dominated, EDLS spectra of water–TBA solutions reported in Figure 1 suggest that water–TBA is an ideal candidate for MD simulations aimed at getting closer to the experimental results and reaching a deeper understanding of the molecular information provided by EDLS spectra.

III.1. Relaxations. At increasing concentration of TBA, a noticeable increase of χ'' in the low frequency part of the spectrum can be observed, similar to what was previously observed for water solutions of several molecules, ranging from carbohydrates^{30,31,44,45} to peptides,^{46,47} amino acids,²⁶ and proteins.^{48,49} Two features emerge from the spectra: the one at about 5 GHz can be assigned to the rotation of solute molecules,^{45,50,51} while the one at about 50 GHz originates from the water molecules whose translational motion is retarded with respect to bulk water.²⁶ A peculiar behavior of water–TBA solutions is that the intensity of the light scattered by TBA rotations is quite low, so that a large part of the signal in the low frequency region of the spectrum can be attributed to the relaxation of retarded (hydration) water.

Consistently with previous studies, the relaxation part of the EDLS spectrum is fitted, as shown in Figure 2, by a phenomenological function given by the sum of a Debye function for the rotational diffusion of TBA and two Cole–Davidson relaxation functions for the contributions of bulk-like and hydration water:

$$\chi''(\omega) = \text{Im}\{-\Delta_{\text{TBA}}[1 + i\omega\tau_{\text{TBA}}]^{-1} - \Delta_{\text{hydr}}[1 + i\omega\tau_{\text{hydr}}]^{-\beta_{\text{hydr}}} - \Delta_{\text{bulk}}[1 + i\omega\tau_{\text{bulk}}]^{-\beta_{\text{bulk}}}\}$$

where Δ_{TBA} , τ_{TBA} , Δ_{hydr} , τ_{hydr} , β_{hydr} and Δ_{bulk} , τ_{bulk} , β_{bulk} are the amplitudes, characteristic times, and shape parameters of TBA rotational diffusion and of the two relaxation processes of water, respectively. Furthermore, since the high frequency side of relaxations extends up to the region where light is scattered also by resonant modes of water and TBA, this part of the spectrum is effectively described by two damped harmonic oscillator

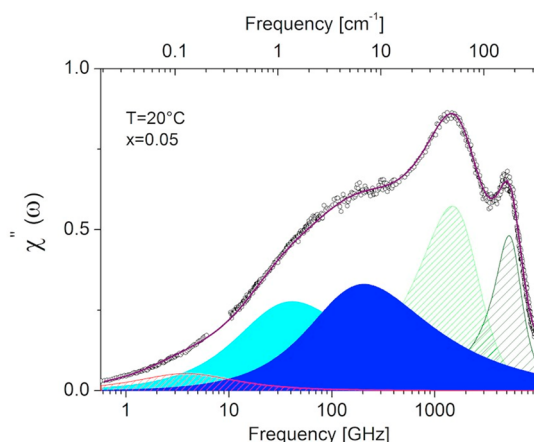


Figure 2. EDLS susceptibility (open symbols) of water–TBA at $x = 0.05$ and $T = 20\text{ }^{\circ}\text{C}$. The total fitting curve (see text) is shown as a solid (purple) line together with the single components: rotational diffusion of TBA (red), relaxation of hydration (blue) and bulk water (cyan), resonant modes of water and TBA (full green and olive lines).

functions.⁴⁶ A more detailed analysis of this region is reported in the next paragraph. Notice that the EDLS spectra are not able to give unambiguous values for the stretching parameters, since the relaxation functions of bulk and hydration water overlap one another and with the H-bond bending and stretching modes. For this reason, the values of the stretching parameters β_{hydr} and β_{bulk} have been fixed at 0.6, the value of pure water, in the whole concentration range. It is worth noticing, as already observed in different aqueous solutions,⁴⁶ that this choice does not influence significantly the concentration behavior of the amplitudes and the ratio of average relaxation times.

Figure 3 shows the values obtained for the relaxation time of the solute.

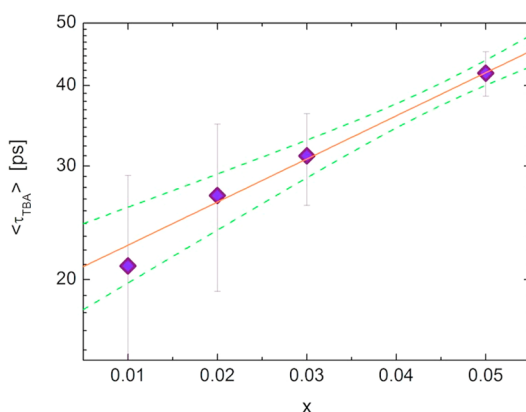


Figure 3. Rotational relaxation time of TBA as a function of solute concentration at $T = 20\text{ }^{\circ}\text{C}$. The solid line represents the Arrhenius behavior, where the logarithm of the relaxation time is proportional to the solute molar fraction; 95% confidence bands are also indicated with dashed lines.

The behavior of τ_{TBA} as a function of x is compatible with an exponential rise that recalls the results previously obtained in glucose–,⁵⁰ trehalose–,⁵¹ and levoglucosan–water⁴⁵ solutions. The behavior can be related to the well-known exponential growth of the viscosity of water solutions with increasing solute content, and the relaxation at $\approx 5\text{ GHz}$ can be associated with

the rotational diffusion of TBA molecules in a medium of increasing viscosity. To correctly interpret our spectra, it is important to notice that EDLS measures the collective reorientational relaxation and that only in the limit of very diluted solutions it provides the single particle correlation time.⁵² As a consequence, in the limit $x \rightarrow 0$, the detected relaxation time can be described by the Stokes–Einstein–Debye (SED) equation, which relates the single particle correlation time to the hydrodynamic volume of the solute V_h and the viscosity of the solution η , through: $\tau_s = V_h \eta / (k_B T)$. By this relation and using the viscosity of water, (1.002 cPoise), we obtain $V_h = 78 \pm 3\text{ \AA}^3$, which is in reasonable agreement with the estimated van der Waals volume of TBA molecules $V_{\text{vdW}} = 86\text{ \AA}^3$.²⁶

Average relaxation times of bulk and hydration water, defined as $\langle \tau \rangle = \beta \tau$, are reported in Figure 4a. It can be seen that

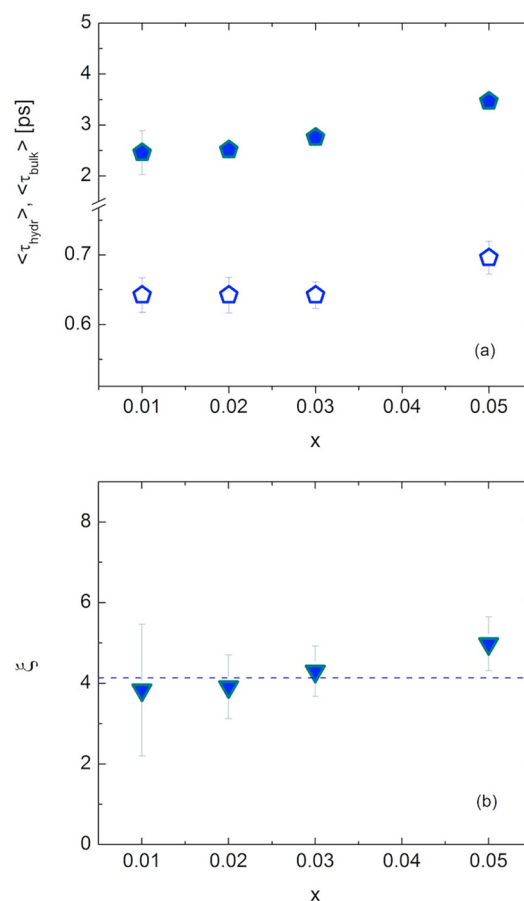


Figure 4. (Upper panel) Average relaxation time of bulk ($\langle \tau_{\text{bulk}} \rangle$) and hydration ($\langle \tau_{\text{hydr}} \rangle$) water and (lower panel) retardation ratio $\xi = \langle \tau_{\text{hydr}} \rangle / \langle \tau_{\text{bulk}} \rangle$ as a function of TBA mole fraction, at $T = 20\text{ }^{\circ}\text{C}$.

$\langle \tau_{\text{bulk}} \rangle$ is very close to that of bulk water (0.65 ps) at $20\text{ }^{\circ}\text{C}$ and very slightly concentration dependent. A possible reason for the increase of $\langle \tau_{\text{bulk}} \rangle$ at the highest investigated concentration can be found in the crudeness of the approximation here adopted in dividing water into two populations, while it would be more reasonable to imagine the existence of a continuous distribution of water molecules more or less perturbed in their motion depending on orientation and distance from one or more solute molecules, especially at the highest solute concentrations.

The average relaxation time of hydration water is also slightly increasing with increasing concentration, so that the retardation

$\xi = \langle \tau_{\text{hydr}} \rangle / \langle \tau_{\text{bulk}} \rangle$ (Figure 4b) is concentration independent, within experimental error, $\xi = 4.1 \pm 0.3$.

It is worth noting that this is one of the smallest values of ξ obtained by EDLS in a number of different solutes,²⁶ with the only exception of levoglucosan.⁴⁵ Nonetheless, this value is about a factor of two higher than that deduced by Brillouin light scattering on the same sample.^{53,54} It should be noted that Brillouin light scattering is a probe of longitudinal viscosity of the solution at the micrometer length scale (hydrodynamic regime), while EDLS, in the case of molecules with almost spherical polarizability, such as water, is predicted to probe density fluctuations at the Angstrom length scale.^{55,56} A wave-vector dependence of the relaxation times⁵⁷ and, possibly, of the retardation factor might explain the difference between the values obtained with the two techniques.

Information on the spatial extent of the perturbation can be obtained from the fraction of water molecules whose dynamics is perturbed with respect to the bulk. The possibility of EDLS to give an estimation of this number (see Figure 5) relies on the assumption that the spectrum can be written as the sum of separate contributions arising from solute and bulk and hydration water, respectively. This important point has been

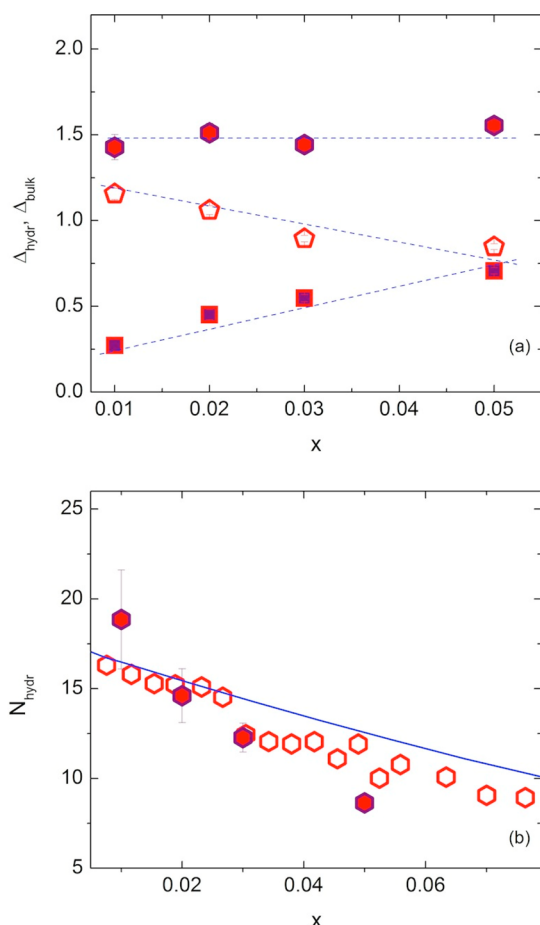


Figure 5. (Upper panel) Amplitude of bulk (squares, Δ_{bulk}) and hydration (pentagons, Δ_{hydr}) relaxation components of water at different TBA concentrations at $T = 20^\circ\text{C}$. The sum of the values of Δ_{bulk} and Δ_{hydr} is also reported (hexagons). (Lower panel) Average hydration number $N_{\text{hydr}} = \Delta_{\text{hydr}}(\Delta_{\text{hydr}} + \Delta_{\text{bulk}})^{-1}(1 - x)/x$. The values previously obtained from molecular dynamics simulation (open symbols)³⁴ and the numerical (solid line) water-sharing model for noninteracting molecules⁵⁸ are also reported for comparison.

recently tested by MD simulations on water–glucose and water–trehalose solutions.^{30,31} It seems reasonable to apply the same analysis to water–TBA solutions, where the anisotropic polarizability of the solute is much lower than that of mono- and disaccharides. Moreover, the sum of the areas of the two water components $\Delta_{\text{bulk}} + \Delta_{\text{hydr}}$ remains almost constant in the whole investigated concentration range (Figure 5a), suggesting that spurious solute–solvent cross terms do not affect the scattering cross section. Under these conditions, the area of the peaks for bulk (Δ_{bulk}) and hydration (Δ_{hydr}) water in Figure 2 is proportional to the fraction of bulk and hydration water molecules, respectively, and the hydration number is obtained by the relationship $N_{\text{hydr}} = \alpha(1 - x)/x$, where $\alpha = \Delta_{\text{hydr}}(\Delta_{\text{hydr}} + \Delta_{\text{bulk}})^{-1}$. This is an intriguing and often underestimated point in spectroscopic investigations, since the desired proportionality between N_{hydr} and α holds true only in the so-called “slow exchange” condition, i.e. for water molecules residing in the bulk and hydration environments for times much longer than that required to relax. In the Appendix we discuss this point in more detail and show that the slow exchange condition is well verified by EDLS, so that the measured relaxation times are, indeed, very close to the hydration and bulk water relaxation times and that the ratio of the peak intensities gives, within experimental error, the values of the hydration number.

Figure 5b shows the values here obtained for N_{hydr} together with those previously estimated by a MD simulation.³⁴ A good agreement is documented between experiments and simulations. Unfortunately, the value of N_{hydr} at the lowest TBA concentration is affected by a very large experimental error. For this reason we prefer to extrapolate the behavior of the other three EDLS data and of MD simulations that, all together, suggest a value of N_{hydr}^0 between 17 and 18 as the average hydration number for a single TBA molecule in the limit $x \rightarrow 0$.

At low concentrations, the reduction of N_{hydr} at increasing solute molar ratio can be understood in terms of water-sharing between hydration shells of close-to-contact molecules. To quantify this effect, we use a recently developed numerical model⁵⁸ where several random configurations of solute molecules are produced in a simulation box with periodic boundary conditions filled by water at the proper density. A typical simulation involves about 27000 molecules of water and a number of solute molecules given by the chosen molar ratio. The TBA molecule is represented by a sphere of volume $V = 78 \text{ \AA}^3$, according to the previously reported hydrodynamic volume. In each configuration, the solute molecules are randomly positioned in the space and replace the water molecules previously filling that volume. After each realization the system is not equilibrated in order to avoid aggregation phenomena induced by any sort of interaction among solutes. The total number of hydration molecules is obtained by counting those within a shell of fixed thickness around at least one solute molecule. The thickness of the shell, 2.5 \AA , is determined by the value of N_{hydr}^0 . The average hydration number N_{hydr} i.e. the total number of hydration molecules divided by the number of solute molecules, is represented in Figure 5b as a continuous line.

The calculated behavior of N_{hydr} compares very well with the MD results at the lowest concentrations ($x < 0.02$). After that, the departure of both MD simulations and EDLS results from the calculated behavior of N_{hydr} suggests that aggregation of TBA molecules occurs at higher solute concentrations. This is in agreement with the results obtained for the resonant modes reported in the next paragraph and with previous investigations performed in water–TBA solutions.⁵⁹

III.2. Resonant Modes. Another important change to the spectrum of water induced by the addition of TBA is visible in Figure 1 as an increase of intensity in the 50 cm^{-1} region, close to the intermolecular H-bond bending mode of water. To better emphasize this effect, in Figure 6 we show the low

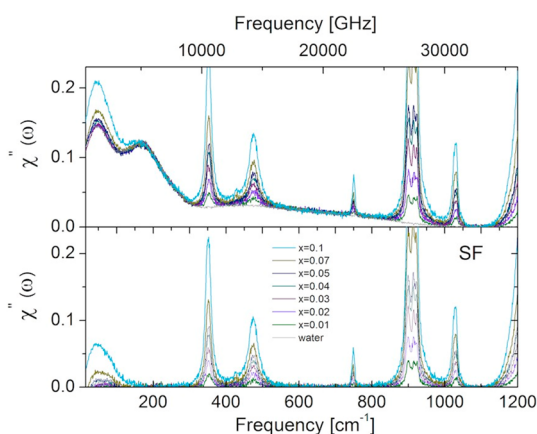


Figure 6. (Upper panel) Low frequency Raman spectra of TBA aqueous solutions at different concentrations. (Lower panel) Solvent free spectra calculated by subtracting the spectrum of pure water from those of the solutions.

frequency depolarized Raman spectra of water–TBA solutions over an extended grid of solute concentrations, namely $x = 0.01; 0.02; 0.03; 0.04; 0.05; 0.07; 0.1$. The spectrum of pure water is also reported, showing the contribution from bending, from stretching, and from the broad librational feature used to normalize all the spectra. After renormalization, an increase of the intensity in the region of the bending mode of water is clearly visible, which is better evidenced in the lower panel of Figure 6 where the solvent free (SF) spectra are reported, obtained by subtracting the spectrum of pure water from those of the solutions.

The asymmetric band at ca. 50 cm^{-1} is typical of many hydrogen-bonding liquids,⁶⁰ including aliphatic alcohols^{61,62} and is generally ascribed to librational motions of the solute molecules.⁶¹ Here, the comparison with the spectrum of pure TBA (Figure 7) confirms this assignment. The idea is that this feature is related to a librational motion of molecules embedded in the local potential minima imposed by their neighbors.⁶³ The inhomogeneous distribution of the frequencies of this motion, primarily responsible for the enlargement of the peak, correlates with the microheterogeneity of the interaction strength. Overall, the effect of TBA hydration is to shift this band toward higher frequencies. The extent of this shift can be quantified by evaluating the average frequency value of the band. Since the spectral feature is asymmetric and extends over more than a hundred cm^{-1} , this can be effectively done by calculating the first moment M_1 of the distribution:

$$M_1 = \frac{\int_{\text{band}} \nu I(\nu) d\nu}{\int_{\text{band}} I(\nu) d\nu}$$

The SF profiles have been integrated in the $15\text{--}135\text{ cm}^{-1}$ frequency range, and the calculated M_1 is reported in the inset of Figure 7.

The behavior of M_1 can be interpreted in terms of intermolecular interactions. In particular, the high values of

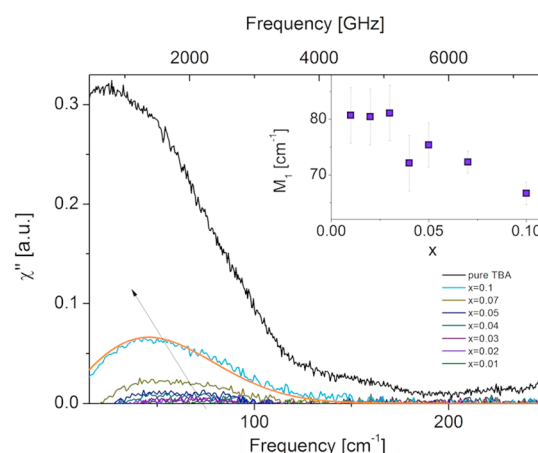


Figure 7. Magnification of the $15\text{--}250\text{ cm}^{-1}$ frequency range of the solvent free Raman spectra. The spectrum of pure TBA is also reported together with the librational antisymmetric component (orange line) given in ref 61. Inset: First spectral moment M_1 of the asymmetric Raman band as a function of the solute molar fraction.

M_1 at low concentrations can be attributed to relatively stiff TBA–water interactions, and the reduction of M_1 for increasing concentration at x greater than ≈ 0.03 can be related to an increasing importance of TBA–TBA interaction due to the aggregation of TBA molecules. A similar effect was observed in the same concentration range by a Raman scattering investigation of the C–H stretching region, around 3000 cm^{-1} ,³ where the high C–H stretching frequencies in the $0\text{--}0.025$ concentration range were connected to the aqueous local environment of the $-\text{CH}_3$ groups and the decreasing trend observed above this regime, with the C–H stretching frequencies tending to the typical values of pure alcohol, was explained in terms of increasing amount of hydrophobic clustering of TBA molecules.

4. CONCLUSIONS

Thanks to the slow-exchange condition that holds for the ps dynamics of water, EDLS can unambiguously reveal the relaxation spectrum of both bulk and hydration water. We find that the dynamics of water molecules involved in the solvation process of TBA is mildly retarded with respect to the bulk. The retardation factor of about 4 resulting from our analysis is one of the lowest obtained by EDLS for a number of biosolutes. A retardation ranging from 5 to 6 was found in mono- and disaccharides,^{30,31,44,48,64} and values up to 8 were found in peptides, amino acids, and protein, with a perturbation extending up to three or more water shells.^{26,46–48,64} The small retardation here obtained for TBA, together with the small number of water molecules perturbed by each TBA molecule, supports the idea that hydrophobic hydration is less effective in perturbing the H-bond network of liquid water.

In very diluted solutions ($x < 0.02$), the reduction of the average hydration number for increasing TBA concentration³⁴ can be explained in terms of a finite probability of finding TBA molecules in a close-to-contact condition. On increasing the concentration over this limit, our results support the idea that TBA molecules start to self-aggregate. Consistently, the first moment M_1 of the spectral band in the $15\text{--}135\text{ cm}^{-1}$ range, related to librational motions of the solute molecules, is almost constant at the lowest TBA concentrations, as expected when the surrounding medium is mostly water. Conversely, for $x >$

0.03 the value of M_1 moves toward lower frequencies, approaching the value measured in pure TBA, as expected for solute molecules that cluster into larger and larger aggregates.

As a whole, TBA has been proven to be a particularly suitable choice for depolarized light scattering studies of aqueous solutions. Because of its low optical anisotropy, most of the signal in the tens of GHz spectral region is due to the relaxation process of water molecules. This system seems to be especially suitable for MD simulations aimed at a better understanding of the molecular origin of depolarized light scattering and its relationship with density fluctuations.

■ APPENDIX

A model that accounts for the relaxation of bulk and hydration water molecules and for the exchange between them was proposed by Anderson⁶⁵ and employed to interpret the dielectric relaxation of different mixtures of water and hydrophobic solutes.^{66–68} According to the model, at any instant the reorientation probability of each water molecule is determined by its local environment. Since the environment around any molecule varies with time, a continuous change in the probability of molecular reorientation. By calling P_B the joint probability that a water molecule is in the bulk environment and has not reoriented and P_H the joint probability that a molecule is in the hydration environment and has not reoriented, their time evolution can be found by solving the coupled rate equations:

$$\begin{aligned}\dot{P}_B(t) &= -(1/\tau_B + kp)P_B(t) + k(1-p)P_H(t) \\ \dot{P}_H(t) &= [1/\tau_H + k(1-p)]P_H(t) + kpP_B(t)\end{aligned}\quad (\text{A1})$$

where $p = N_H x / (1 - x)$ is the mole fraction of hydration water and kp and $k(1-p)$ are the rate constants for the transfer from B to H and from H to B, respectively, with N_H the hydration number. After solving these equations, one obtains the relaxation functions measured by the experiment, with relaxation times τ_{hydr} and τ_{bulk} linked to τ_B , τ_H , and k by the relation

$$\begin{aligned}1/\tau_{\text{hydr,bulk}} &= 1/2(1/\tau_B + 1/\tau_H + k) \\ \mp 1/2[(1/\tau_B - 1/\tau_H - k)^2 + 4kp(1/\tau_B - 1/\tau_H)]^{1/2}\end{aligned}\quad (\text{A2})$$

The relative amplitudes of the bulk and hydration relaxation processes are given as α and $1 - \alpha$, where α is given by the equation

$$\alpha = [1/\tau_{\text{bulk}} - p/\tau_H - (1-p)/\tau_B] / (1/\tau_{\text{bulk}} - 1/\tau_{\text{hydr}}) \quad (\text{A3})$$

This scheme was proven to correctly describe the dielectric relaxation of water–alcohol solutions,^{66–68} with a value for the exchange rate that is close to those of the dielectric relaxation rates. In that case, one measures a seeming increase of the retardation ξ ⁶⁷ with values of τ_{bulk} that stay quite constant and close to τ_B and values of τ_{hydr} that increase with increasing solute concentration, approaching the value of τ_H when the residual fraction of bulk water tends to zero. Interestingly, this mechanism could also explain the concentration dependence of ξ recently reported by a dielectric spectroscopy investigation of water TMU solutions¹⁴ and could explain the seeming increase of ξ in terms of bulk–hydration water exchange, similar to what was found in ref 67.

The physical picture behind this simple kinetic model is quite general and can be applied to different physical observables. In fact, also in the case of solvation dynamics revealed by femtosecond fluorescence techniques,^{69,70} the dynamics of water molecules was described by a similar approach, with the hypothesis $1/\tau_H = 0$, i.e. supposing that the diffusion time of hydration molecules is much higher than the exchange rate (see ref 71, eqs A3), so that the relaxation of hydration water can occur only via exchange with bulk water.

Two other important limiting cases are represented by the conditions $k \gg 1/\tau_B$, $1/\tau_H$ and $k \ll 1/\tau_B$, $1/\tau_H$, corresponding to an exchange rate that is very fast and very slow with respect to the relaxation rates.

The first condition gives rise to a single measurable relaxation process with a relaxation rate that is the weighted average of those of hydration and bulk water, as in NMR experiments.

The second condition corresponds to a more “ideal” scenario, where hydration molecules reside close to the solute molecule for a time very long with respect to the relaxation time. In this case, the measured relaxation times coincide with those of hydration and bulk water $\tau_{\text{hydr}} = \tau_H$, $\tau_{\text{bulk}} = \tau_B$, and the amplitudes of the two relaxations are proportional to the relative fraction of water molecules, i.e. $\alpha = p$. This is the condition that more closely applies to our EDLS experiments.

In fact, estimations of the exchange times obtained by a wide variety of techniques give values of k^{-1} ranging from ≈ 30 to ≈ 10 ps. Values close to 30 ps are obtained by dielectric relaxation in water–TBA solutions⁶⁷ when rescaled at 20 °C, as well as from MD simulations of the second-rank rotational relaxation of water molecules on protein solutions,^{72,73} consistent with the average time taken by a hydrating water molecule to move away from the protein surface of 3 Å (ca. one water diameter).⁷³ Using the same procedure for small hydrophobic molecules, such as TMAO and TMU, and rotational perturbation factors $\xi = 1.6$ resulting from NMR experiments,²³ residence times of about 10 ps can be derived, in agreement with the average time needed by a water molecule to cover a distance of 3 Å in diluted solutions of the same hydrophobes.⁷⁴ Note that rotational ξ values more than four times greater than this have been obtained by ultrafast infrared experiments^{12,13} such that residence times significantly exceeding 10 ps would be inferred. In summary, if we take the upper value $k^{-1} = 30$, and τ_{hydr} and τ_{bulk} from our results in Figure 4a, by the numerical inversion of eqs A2 and A3 a difference less than 8% is found in the values of τ_H and τ_B with respect to τ_{hydr} and τ_{bulk} and less than 2% in the value of N_h with respect to N_{hydr} . On the other hand, if we take the lower value $k^{-1} = 10$ ps, a difference less than 18% is found in the values of τ_H and τ_B and less than 10% in the value of N_h . In both cases, these results confirm that, for our EDLS data, within experimental errors, $\tau_{\text{hydr}} \approx \tau_H$, $\tau_{\text{bulk}} \approx \tau_B$, and $\alpha \approx p$, i.e. $N_{\text{hydr}} \approx N_H$.

■ AUTHOR INFORMATION

Corresponding Author

*E-mail: daniele.fioretto@fisica.unipg.it.

Notes

The authors declare no competing financial interest.

■ ACKNOWLEDGMENTS

S.C. acknowledges support from MIUR-PRIN (Project 2012J8X57P). M.P. acknowledges support from MIUR-PRIN 2010–2011.

REFERENCES

- (1) Ball, P. Water as an Active Constituent in Cell Biology. *Chem. Rev.* **2008**, *108*, 74–108.
- (2) Davis, J. G.; Gierszal, K. P.; Wang, P.; Ben-Amotz, D. Water Structural Transformation at Molecular Hydrophobic Interfaces. *Nature* **2012**, *491*, 582–585.
- (3) Di Michele, A.; Freda, M.; Onori, G.; Paolantoni, M.; Santucci, A.; Sassi, P. Modulation of Hydrophobic Effect by Cosolutes. *J. Phys. Chem. B* **2006**, *110*, 21077–21085.
- (4) Sinibaldi, R.; Casieri, C.; Melchionna, S.; Onori, G.; Segre, A. L.; Viel, S.; Mannina, L.; De Luca, F. The Role of Water Coordination in Binary Mixtures. A Study of Two Model Amphiphilic Molecules in Aqueous Solutions by Molecular Dynamics and NMR. *J. Phys. Chem. B* **2006**, *110*, 8885–8892.
- (5) Wilcox, D. S.; Rankin, B. M.; Ben-Amotz, D. Distinguishing Aggregation From Random Mixing in Aqueous T-Butyl Alcohol Solutions. *Faraday Discuss.* **2013**, *167*, 177.
- (6) Soper, A. K.; Finney, J. L. Hydration of Methanol in Aqueous Solution. *Phys. Rev. Lett.* **1993**, *71*, 4346–4349.
- (7) Dixit, S.; Crain, J.; Poon, W. C. K.; Finney, J. L.; Soper, A. K. Molecular Segregation Observed in a Concentrated Alcohol–Water Solution. *Nature* **2002**, *416*, 829–832.
- (8) Tomlinson-Phillips, J.; Davis, J.; Ben-Amotz, D.; Spångberg, D.; Pejov, L.; Hermansson, K. Structure and Dynamics of Water Dangling OH Bonds in Hydrophobic Hydration Shells. Comparison of Simulation and Experiment. *J. Phys. Chem. A* **2011**, *115*, 6177–6183.
- (9) Galamba, N. Water's Structure Around Hydrophobic Solutes and the Iceberg Model. *J. Phys. Chem. B* **2013**, *117*, 2153–2159.
- (10) Fidler, J.; Rodger, P. M. Solvation Structure Around Aqueous Alcohols. *J. Phys. Chem. B* **1999**, *103*, 7695–7703.
- (11) Banerjee, S.; Furtado, J.; Bagchi, B. Fluctuating Micro-Heterogeneity in Water–Tert-Butyl Alcohol Mixtures and Lambda-Type Divergence of the Mean Cluster Size with Phase Transition-Like Multiple Anomalies. *J. Chem. Phys.* **2014**, *140*, 194502.
- (12) Petersen, C.; Tielrooij, K. J.; Bakker, H. J. Strong Temperature Dependence of Water Reorientation in Hydrophobic Hydration Shells. *J. Chem. Phys.* **2009**, *130*, 214511.
- (13) Bakulin, A. A.; Pshenichnikov, M. S.; Bakker, H. J.; Petersen, C. Hydrophobic Molecules Slow Down the Hydrogen-Bond Dynamics of Water. *J. Phys. Chem. A* **2011**, *115*, 1821–1829.
- (14) Tielrooij, K.-J.; Hunger, J.; Buchner, R.; Bonn, M.; Bakker, H. J. Influence of Concentration and Temperature on the Dynamics of Water in the Hydrophobic Hydration Shell of Tetramethylurea. *J. Am. Chem. Soc.* **2010**, *132*, 15671–15678.
- (15) Titantah, J. T.; Karttunen, M. Long-Time Correlations and Hydrophobe-Modified Hydrogen-Bonding Dynamics in Hydrophobic Hydration. *J. Am. Chem. Soc.* **2012**, *134*, 9362–9368.
- (16) Duboué-Dijon, E.; Fogarty, A. C.; Laage, D. Temperature Dependence of Hydrophobic Hydration Dynamics: From Retardation to Acceleration. *J. Phys. Chem. B* **2014**, *118*, 1574–1583.
- (17) Silvestrelli, P. L. Are There Immobilized Water Molecules Around Hydrophobic Groups? Aqueous Solvation of Methanol From First Principles. *J. Phys. Chem. B* **2009**, *113*, 10728–10731.
- (18) Rossato, L.; Rossetto, F.; Silvestrelli, P. L. Aqueous Solvation of Methane From First Principles. *J. Phys. Chem. B* **2012**, *116*, 4552–4560.
- (19) Laage, D.; Stirnemann, G.; Hynes, J. T. Why Water Reorientation Slows Without Iceberg Formation Around Hydrophobic Solutes. *J. Phys. Chem. B* **2009**, *113*, 2428–2435.
- (20) Nakahara, M.; Wakai, C.; Yoshimoto, Y.; Matubayasi, N. Dynamics of Hydrophobic Hydration of Benzene. *J. Phys. Chem.* **1996**, *100*, 1345–1349.
- (21) Ishihara, Y.; Okouchi, S.; Uedaira, H. Dynamics of Hydration of Alcohols and Diols in Aqueous Solutions. *Faraday Trans.* **1997**, *93*, 3337–3342.
- (22) Yoshida, K.; Ibuki, K.; Ueno, M. Pressure and Temperature Effects on [Sup 2]H Spin-Lattice Relaxation Times and [Sup 1]H Chemical Shifts in Tert-Butyl Alcohol- and Urea-D[Sub 2]O Solutions. *J. Chem. Phys.* **1998**, *108*, 1360–1367.
- (23) Qvist, J.; Halle, B. Thermal Signature of Hydrophobic Hydration Dynamics. *J. Am. Chem. Soc.* **2008**, *130*, 10345–10353.
- (24) Li, G.; Du, W. M.; Chen, X. K.; Cummins, H. Z.; Tao, N. J. Testing Mode-Coupling Predictions for A and B Relaxation in Ca 0.4 K 0.6 (NO 3) 1.4 Near the Liquid-Glass Transition by Light Scattering. *Phys. Rev. A* **1992**, *45*, 3867.
- (25) Fukasawa, T.; Sato, T.; Watanabe, J.; Hama, Y.; Kunz, W.; Buchner, R. Relation Between Dielectric and Low-Frequency Raman Spectra of Hydrogen-Bond Liquids. *Phys. Rev. Lett.* **2005**, *95*, No. 197802EP.
- (26) Comez, L.; Lupi, L.; Morresi, A.; Paolantoni, M.; Sassi, P.; Fioretto, D. More Is Different: Experimental Results on the Effect of Biomolecules on the Dynamics of Hydration Water. *J. Phys. Chem. Lett.* **2013**, *4*, 1188–1192.
- (27) Geiger, L. C.; Ladanyi, B. M. Molecular Dynamics Simulation Study of Nonlinear Optical Response of Fluids. *Chem. Phys. Lett.* **1989**, *159*, 413–420.
- (28) Paolantoni, M.; Sassi, P.; Morresi, A.; Santini, S. Hydrogen Bond Dynamics and Water Structure in Glucose-Water Solutions by Depolarized Rayleigh Scattering and Low-Frequency Raman Spectroscopy. *J. Chem. Phys.* **2007**, *127*, No. 024504.
- (29) Elola, M. D.; Ladanyi, B. M. Intermolecular Polarizability Dynamics of Aqueous Formamide Liquid Mixtures Studied by Molecular Dynamics Simulations. *J. Chem. Phys.* **2007**, *126*, 084504.
- (30) Lupi, L.; Comez, L.; Paolantoni, M.; Fioretto, D.; Ladanyi, B. M. Dynamics of Biological Water: Insights From Molecular Modeling of Light Scattering in Aqueous Trehalose Solutions. *J. Phys. Chem. B* **2012**, *116*, 7499–7508.
- (31) Lupi, L.; Comez, L.; Paolantoni, M.; Perticaroli, S.; Sassi, P.; Morresi, A.; Ladanyi, B. M.; Fioretto, D. Hydration and Aggregation in Mono- and Disaccharide Aqueous Solutions by Gigahertz-to-Terahertz Light Scattering and Molecular Dynamics Simulations. *J. Phys. Chem. B* **2012**, *116*, 14760–14767.
- (32) Fukasawa, T.; Tominaga, Y.; Wakisaka, A. Molecular Association in Binary Mixtures of Tert-Butyl Alcohol–Water and Tetrahydrofuran–Heavy Water Studied by Mass Spectrometry of Clusters From Liquid Droplets. *J. Phys. Chem. A* **2004**, *108*, 59–63.
- (33) Freda, M.; Onori, G.; Santucci, A. Infrared Study of the Hydrophobic Hydration and Hydrophobic Interactions in Aqueous Solutions of Tert-Butyl Alcohol and Trimethylamine- N-Oxide. *J. Phys. Chem. B* **2001**, *105*, 12714–12718.
- (34) Fornili, A.; Civera, M.; Sironi, M.; Fornili, S. L. Molecular Dynamics Simulation of Aqueous Solutions of Trimethylamine-N-Oxide and Tert-Butyl Alcohol. *Phys. Chem. Chem. Phys.* **2003**, *5*, 4905.
- (35) Bender, T. M.; Pecora, R. A Dynamic Light Scattering Study of the Tert-Butyl Alcohol-Water System. *J. Phys. Chem.* **1986**, *90*, 1700–1706.
- (36) Petersen, C.; Bakulin, A. A.; Pavelyev, V. G.; Pshenichnikov, M. S.; Bakker, H. J. Femtosecond Midinfrared Study of Aggregation Behavior in Aqueous Solutions of Amphiphilic Molecules. *J. Chem. Phys.* **2010**, *133*, 164514.
- (37) Comez, L.; Masciovecchio, C.; Monaco, G.; Fioretto, D. Progress in Liquid and Glass Physics by Brillouin Scattering Spectroscopy. In *Solid State Physics; Solid State Physics*; Elsevier: **2012**; Vol. 63, pp 1–77.
- (38) Paolantoni, M.; Comez, L.; Fioretto, D.; Gallina, M. E.; Morresi, A.; Sassi, P.; Scarponi, F. Structural and Dynamical Properties of Glucose Aqueous Solutions by Depolarized Rayleigh Scattering. *J. Raman Spectrosc.* **2008**, *39*, 238–243.
- (39) Faurskov Nielsen, O. Low-Frequency Spectroscopic Studies and Intermolecular Vibrational Energy Transfer in Liquids. *Annu. Rep. Prog. Chem., Sect. C* **1997**, *93*, 57–99.
- (40) Sokolov, A.; Hurst, J.; Quitmann, D. Dynamics of Supercooled Water: Mode-Coupling Theory Approach. *Phys. Rev. B* **1995**, *51*, 12865–12868.
- (41) Sonoda, M. T.; Vecchi, S. R. M.; Skaf, M. S. A Simulation Study of the Optical Kerr Effect in Liquid Water. *Phys. Chem. Chem. Phys.* **2005**, *7*, 1176.

- (42) Martin, D. R.; Fioretto, D.; Matyushov, D. V. Depolarized Light Scattering and Dielectric Response of a Peptide Dissolved in Water. *J. Chem. Phys.* **2014**, *140*, No. 035101.
- (43) Martin, D. R.; Matyushov, D. V. Hydration Shells of Proteins Probed by Depolarized Light Scattering and Dielectric Spectroscopy: Orientational Structure Is Significant, Positional Structure Is Not. *J. Chem. Phys.* **2014**, *141*, 22D501.
- (44) Paolantoni, M.; Comez, L.; Gallina, M. E.; Sassi, P.; Scarponi, F.; Fioretto, D.; Morresi, A. Light Scattering Spectra of Water in Trehalose Aqueous Solutions: Evidence for Two Different Solvent Relaxation Processes. *J. Phys. Chem. B* **2009**, *113*, 7874–7878.
- (45) Corezzi, S.; Sassi, P.; Paolantoni, M.; Comez, L.; Morresi, A.; Fioretto, D. Hydration and Rotational Diffusion of Levoglucosan in Aqueous Solutions. *J. Chem. Phys.* **2014**, *140*, 184505.
- (46) Perticaroli, S.; Comez, L.; Paolantoni, M.; Sassi, P.; Morresi, A.; Fioretto, D. Extended Frequency Range Depolarized Light Scattering Study of N-Acetyl-Leucine-Methylamide–Water Solutions. *J. Am. Chem. Soc.* **2011**, *133*, 12063–12068.
- (47) Comez, L.; Perticaroli, S.; Paolantoni, M.; Sassi, P.; Corezzi, S.; Morresi, A.; Fioretto, D. Concentration Dependence of Hydration Water in a Model Peptide. *Phys. Chem. Chem. Phys.* **2014**, *16*, 12433.
- (48) Perticaroli, S.; Comez, L.; Paolantoni, M.; Sassi, P.; Lupi, L.; Fioretto, D.; Paciaroni, A.; Morresi, A. Broadband Depolarized Light Scattering Study of Diluted Protein Aqueous Solutions. *J. Phys. Chem. B* **2010**, *114*, 8262–8269.
- (49) Perticaroli, S.; Comez, L.; Sassi, P.; Paolantoni, M. Hydration and Aggregation of Lysozyme by Extended Frequency Range Depolarized Light Scattering. *J. Non-Cryst. Solids* **2015**, *407*, 472–477.
- (50) Fioretto, D.; Comez, L.; Gallina, M. E.; Morresi, A.; Palmieri, L.; Paolantoni, M.; Sassi, P.; Scarponi, F. Separate Dynamics of Solute and Solvent in Water–Glucose Solutions by Depolarized Light Scattering. *Chem. Phys. Lett.* **2007**, *441*, 232–236.
- (51) Gallina, M. E.; Comez, L.; Morresi, A.; Paolantoni, M.; Perticaroli, S.; Sassi, P.; Fioretto, D. Rotational Dynamics of Trehalose in Aqueous Solutions Studied by Depolarized Light Scattering. *J. Chem. Phys.* **2010**, *132*, 214508.
- (52) Kivelson, D.; Madden, P. A. Light Scattering Studies of Molecular Liquids. *Annu. Rev. Phys. Chem.* **1980**, *31*, 523–558.
- (53) Lupi, L.; Comez, L.; Masciovecchio, C.; Morresi, A.; Paolantoni, M.; Sassi, P.; Scarponi, F.; Fioretto, D. Hydrophobic Hydration of Tert-Butyl Alcohol Studied by Brillouin Light and Inelastic Ultraviolet Scattering. *J. Chem. Phys.* **2011**, *134*, 055104.
- (54) Comez, L.; Lupi, L.; Paolantoni, M.; Picchiò, F.; Fioretto, D. Hydration Properties of Small Hydrophobic Molecules by Brillouin Light Scattering. *J. Chem. Phys.* **2012**, *137*, 114509.
- (55) Tao, N. J.; Li, G.; Chen, X.; Du, W. M.; Cummins, H. Z. Low-Frequency Raman-Scattering Study of the Liquid-Glass Transition in Aqueous Lithium Chloride Solutions. *Phys. Rev. A* **1991**, *44*, 6665–6676.
- (56) Stephen, M. J. Raman Scattering in Liquid Helium. *Phys. Rev.* **1969**, *187*, 279–285.
- (57) Chen, S. H.; Gallo, P.; Sciortino, F.; Tartaglia, P. Molecular-Dynamics Study of Incoherent Quasielastic Neutron-Scattering Spectra of Supercooled Water. *Phys. Rev. E* **1997**, *56*, 4231.
- (58) Fioretto, D.; Comez, L.; Corezzi, S.; Paolantoni, M.; Sassi, P.; Morresi, A. Solvent Sharing Models for Non-Interacting Solute Molecules: the Case of Glucose and Trehalose Water Solutions. *Food Biophysics* **2013**, *8*, 177–182.
- (59) Di Michele, A.; Freda, M.; Onori, G.; Santucci, A. Hydrogen Bonding of Water in Aqueous Solutions of Trimethylamine-N-Oxide and Tert-Butyl Alcohol: a Near-Infrared Spectroscopy Study. *J. Phys. Chem. A* **2004**, *108*, 6145–6150.
- (60) Hunt, N. T.; Turner, A. R.; Wynne, K. Inter- and Intramolecular Hydrogen Bonding in Phenol Derivatives: a Model System for Poly- L-Tyrosine. *J. Phys. Chem. B* **2005**, *109*, 19008–19017.
- (61) Sassi, P.; Paolantoni, M.; Perticaroli, S.; Palombo, F.; Morresi, A. A Study of Collective Motions in Liquid Tert-Butanol From Low-Wavenumber Raman Scattering. *J. Raman Spectrosc.* **2009**, *40*, 1279–1283.
- (62) Smith, N. A.; Meech, S. R. Femtosecond Polarizability Anisotropy Relaxation and Solvation Dynamics the Cases of Aniline and Methanol. *Faraday Discuss.* **1997**, *108*, 35–50.
- (63) Lynden-Bell, R. M.; Steele, W. A. A Model for Strongly Hindered Molecular Reorientation in Liquids. *J. Phys. Chem.* **1984**, *88*, 6514–6518.
- (64) Perticaroli, S.; Nakanishi, M.; Pashkovski, E.; Sokolov, A. P. Dynamics of Hydration Water in Sugars and Peptides Solutions. *J. Phys. Chem. B* **2013**, *117*, 7729–7736.
- (65) Anderson, J. E. Time-Dependent Reorientation Probabilities and Molecular Relaxation. *J. Chem. Phys.* **1967**, *47*, 4879–4883.
- (66) Hallenga, K.; Grigera, J. R.; Berendsen, H. J. C. Influence of Hydrophobic Solutes on the Dynamic Behavior of Water. *J. Phys. Chem.* **1980**, *84*, 2381–2390.
- (67) Fioretto, D.; Marini, A.; Massarotti, M.; Onori, G.; Palmieri, L.; Santucci, A.; Socino, G. Dielectric Relaxation in Water-Tert-Butanol Mixtures. the Water Rich Region. *J. Chem. Phys.* **1993**, *99*, 8115–8119.
- (68) Fioretto, D.; Marini, A.; Onori, G.; Palmieri, L.; Santucci, A.; Socino, G.; Verdini, L. Study of Aggregation in Water—N-Butoxyethanol Solutions by Dielectric Relaxation Measurements. *Chem. Phys. Lett.* **1992**, *196*, 583–587.
- (69) Pal, S. K.; Zewail, A. H. Dynamics of Water in Biological Recognition. *Chem. Rev.* **2004**, *104*, 2099–2124.
- (70) Pal, S. K. Biological Water at the Protein Surface: Dynamical Solvation Probed Directly with Femtosecond Resolution. *Proc. Natl. Acad. Sci. U. S. A.* **2002**, *99*, 1763–1768.
- (71) Pal, S. K.; Peon, J.; Bagchi, B.; Zewail, A. H. Biological Water: Femtosecond Dynamics of Macromolecular Hydration. *J. Phys. Chem. B* **2002**, *106*, 12376–12395.
- (72) Marchi, M.; Sterpone, F.; Ceccarelli, M. Water Rotational Relaxation and Diffusion in Hydrated Lysozyme. *J. Am. Chem. Soc.* **2002**, *124*, 6787–6791.
- (73) Pizzitutti, F.; Marchi, M.; Sterpone, F.; Rossky, P. J. How Protein Surfaces Induce Anomalous Dynamics of Hydration Water. *J. Phys. Chem. B* **2007**, *111*, 7584–7590.
- (74) Stirnemann, G.; Sterpone, F.; Laage, D. Dynamics of Water in Concentrated Solutions of Amphiphiles: Key Roles of Local Structure and Aggregation. *J. Phys. Chem. B* **2011**, *115*, 3254–3262.